Assessing the Relationship between Forest Proportion, Soil Moisture Index and Net Primary Productivity in Pa Sak Ngam, Chiang Mai Province, Thailand

Namwong, C.,[1] Suwanprasit, C.,[1*] Shahnawaz, S.[2] and Wongpornchai, P.[3]
[1]Department of Geography, Faculty of Social Sciences, Chiang Mai University 50200, Thailand
E-mail: chakkaphong.nw@gmail.com, chanida.suwanprasit@gmail.com*
[2]Interfaculty Department for Geoinformatics–Z_GIS, University of Salzburg, 5020 Salzburg, Austria
E-mail: s.shahnawaz@sbg.ac.at
[3]Department of Geological Sciences, Faculty of Science, Chiang Mai University 50200, Thailand
E-mail: pisanu.w@cmu.ac.th
**Corresponding Author*

DOI: https://doi.org/10.52939/ijg.v19i2.2563

Abstract
The objective of this study was to determine the relationship between the proportion of forest area, soil moisture index, and net primary productivity in the Pa Sak Ngam, Luang Nuea Subdistrict, Doi Saket District Chiang Mai, Thailand. The investigation was conducted during dry season in 2009 and 2019 utilizing systematic sampling inside a 500 m × 500 m image grid to measure these factors. Landsat 5 TM and Landsat 8 OLI/TIRS satellite images were classified using the Random Forest to obtain the proportion of forest area. Soil moisture was calculated using the soil moisture index obtained from land surface temperature and the normalized difference vegetation index. The Physiological Processes Predicting Growth (3-PGs) model was used to compute net primary productivity. In 2009, the analysis revealed a moderately strong positive correlation between the proportion of forest area and both soil moisture and net primary productivity. In contrast, in 2019, a weak positive association was found between low forest cover percentage and both soil moisture and net primary productivity. A comparison of the results from the two time periods indicated that the association between the three variables was stronger in 2009 than in 2019. This may be attributed to the increase in average forest cover from 85.583% to 92.349% over the two time periods. Effective management of forest restoration and expansion can enhance the water cycle and increase the flow of energy and productivity.

Keywords: 3-PGs; Forest Proportion; Net Primary Productivity; Random Forest; Soil Moisture Index

1. Introduction

Net Primary Productivity (NPP), Gross Primary Productivity (GPP), or Net Ecosystem Productivity (NEP) are three different measures of the productivity of an ecosystem, and they are all linked to forest health and soil moisture in different ways. As defined by [1] NPP represents the amount of carbon fixed by plants through photosynthesis, which is directly related to the growth and productivity of vegetation. NPP is therefore a direct measure of the amount of energy that is available for higher trophic levels in the ecosystem, including herbivores and predators. Additionally, NPP is a useful indicator of ecosystem health and function, as it reflects the balance between carbon uptake and carbon release by an ecosystem. In contrast, NEP represents the net carbon exchange between the ecosystem and the atmosphere and is influenced by both GPP and ecosystem respiration. While NEP can be a useful indicator of carbon sequestration and ecosystem carbon balance, it is not as directly related to vegetation productivity and health as NPP.

Similarly, GPP represents the total amount of carbon fixed by plants but does not consider the amount of carbon respired by plants during cellular respiration. This can lead to an overestimation of carbon uptake and productivity. Several studies have shown that NPP is a more accurate indicator of forest health than NEP or GPP, as it directly measures plant growth and productivity. For example, [2] used satellite-based estimates of NPP

to evaluate the impact of drought on forest health in West Africa and found that NPP was a more reliable indicator of vegetation response to drought than NEP or GPP. Similarly, a study by [3] used long-term measurements of NPP to assess the impact of climate change on forest health in China and found that changes in NPP were closely correlated with changes in forest productivity and health.

The relationship between NPP and soil moisture is a complex one, as the availability of water can have both positive and negative effects on plant growth and productivity. Adequate soil moisture is necessary for optimal plant growth and NPP. When soil moisture is sufficient, plants are able to take up enough water to support photosynthesis and growth. However, when soil moisture is too high, oxygen levels in the soil can become limiting, negatively affecting plant growth and NPP. On the other hand, when soil moisture is too low, plants can become stressed and may not be able to take up enough water to support photosynthesis, which can reduce NPP [4].

Also, low soil moisture can lead to water and heat stress on plants, affecting their growth and productivity [4] and [5]. Alterations in soil moisture patterns can significantly impact the functioning of forest ecosystems. Factors such as changes in forest cover ratio and NPP can mediate these changes in soil moisture patterns, leading to variations in forest stand dynamics. For example, a decrease in forest cover ratio can reduce the amount of vegetation present to transpire water and shade the soil, reducing soil moisture. Similarly, a decrease in NPP can reduce the amount of organic matter being produced and returned to the soil, leading to changes in soil structure and nutrient availability that can affect soil moisture levels [6] and [7]. These changes in soil moisture patterns can also have a cascading effect on other ecosystem processes. For example, soil moisture changes can affect water availability for plant growth and photosynthesis, which can impact NPP. Additionally, soil moisture changes can affect water availability for other organisms, such as insects, fungi, and microorganisms, which can impact the overall biodiversity of the ecosystem [8].

Several recent studies have used the Physiological Principles Predicting Growth (3-PG) model in conjunction with remote sensing to estimate NPP in different ecosystems. The 3-PG model is a process-based model that simulates the growth of plants by taking into account various physiological and environmental factors, such as temperature, precipitation, solar radiation, and leaf area index (LAI) [9] [10] and [11].

Additionally, the 3-PG model provides a reliable method for assessing how hydrology and soil water availability affect the growth of different forest species. Later, the 3-PG was incorporated into satellite images and became the 3-PGS (Physiological Principles for Predicting Growth from Satellites) [12] and [13].

Soil moisture estimation through remote sensing includes various techniques that use visible and microwave bands. Soil Moisture Index (SMI) is defined as the proportion of the difference between the current soil moisture and the permanent wilting point to the field capacity and the residual soil moisture [14]. While microwave methods can be used at night and in cloudy conditions, optical and thermal methods are also important for sensing soil moisture, particularly because they can produce high-resolution maps. The Normalized Difference Vegetation Index (NDVI) and Land Surface Temperature (LST) are two remote sensing-based parameters that have been used to estimate soil moisture recently. Many researchers have shown a negative correlation between Vegetation Index (VI) and LST at various spatial scales [15] [16] and [17]. This study aimed to determine the percentage of forest in the Mae Khung Basin of Chiang Mai Province, Thailand, using a grid-based method together with Random Forest (RF) Classifier. Additionally, we examined the relationship between the forest proportion, soil moisture, and NPP from the 3-PG model from 2009 to 2019.

2. Study Area

The Ban Pa Sak Ngam (Figure 1) is a village which is located in the Mae Khung Basin in Chiang Mai Province, Thailand and is surrounded by national forest reserves (Longitude of 19.0016° N and Latitude of 99.1335° E). The area of Ban Pa Sak Ngam is approximately 112 km^2, with a residential area of 0.8 km^2. The village is located in a watershed that supplies water to the Mae Khung Udom Thara Reservoir and is part of the Khun Mae Kuang Forest Development Project, a Royal Initiative aimed at restoring and protecting the forested area.

Before the government granted forest concessions to commercial agencies, Pa Sak Ngam Village had a rich forest community. However, giving these concessions led to the degradation of the watershed forests, the depletion of water sources from the local waterfalls, and a decline in forest diversity. In response to these issues, efforts have been made to plant forests and educate the local community about the importance of forest conservation [18].

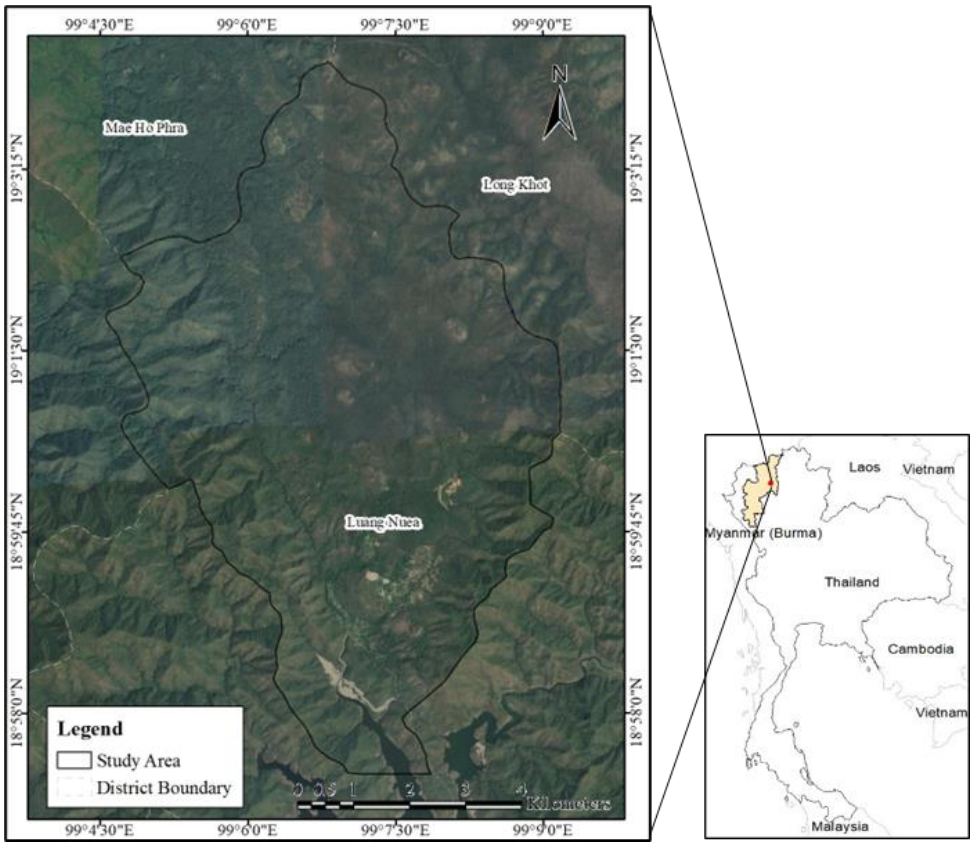

Figure 1: The study area

As a result, Pa Sak Ngam is an ideal location for studying the condition of the forest during its restoration and the current state of the ecosystem. Researchers can examine the relationship between ecological restoration management variables (such as the proportion of forest area) and key ecological natural variables (such as SMI and NPP) to understand the current conditions of the ecosystem better.

3. Data and Methods

3.1 Data

The study used 30 m resolution Landsat 5 TM and Landsat 8OLI/TIRS satellite image data of January 2009 and 2019 obtained from the United States Geological Survey (USGS) Earth Explorer website (*https://earthexplorer.usgs.gov/*) to generate land cover, SMI, and NPP. The total rainfall data for the study area in Thailand was obtained from three government agencies: the Meteorological Department, the Royal Irrigation Department, and the Department of Water Resource. The data was collected from 16 stations in 2008 and 22 stations in 2018 (Figure 2). This data was used to summarize the rainfall in the study area and generate precipitation estimates using the Inverse Distance Weighting (IDW) interpolation method which uses the inverse distance as a weighting factor and depends on the cartesian quarters of the target station. The interpolated values are related to the value of the surrounding reference points. The IDW approach is widely recognized as the basic technique for spatial rainfall interpolation since it is easier, faster, and more accurate than other methods [19] [20] and [21] (Figure 3).

3.2 Methods

Firstly, Landsat 5 TM and Landsat 8 OLI/TIRS images from January 2009 and January 2019, respectively, were obtained and pre-processed. Subsequently, the multispectral bands were classified using the RF classifier to ascertain the percentage of forest cover, which was validated against the existing Landuse data from the Land Development Department for both years. The RF classifier is a classification method based on machine learning which have gained popularity because of its ability to classify data while processing it quickly and accurately [22] [23] [24] and [25]. The concept of RF is to create a group of decision trees and merges their outcomes to categorize new data points. To minimize overfitting,

a major issue with decision trees, the forest is trained on random subsets and attributes of data [26]. Afterward, LST and NDVI were calculated to determine the SMI. In addition, NPP was calculated using the 3-PGs model.

Finally, the relationship between these parameters was analyzed using grid-based values within a 500 m x 500 m area. The process outlined in the study is illustrated in Figure 4.

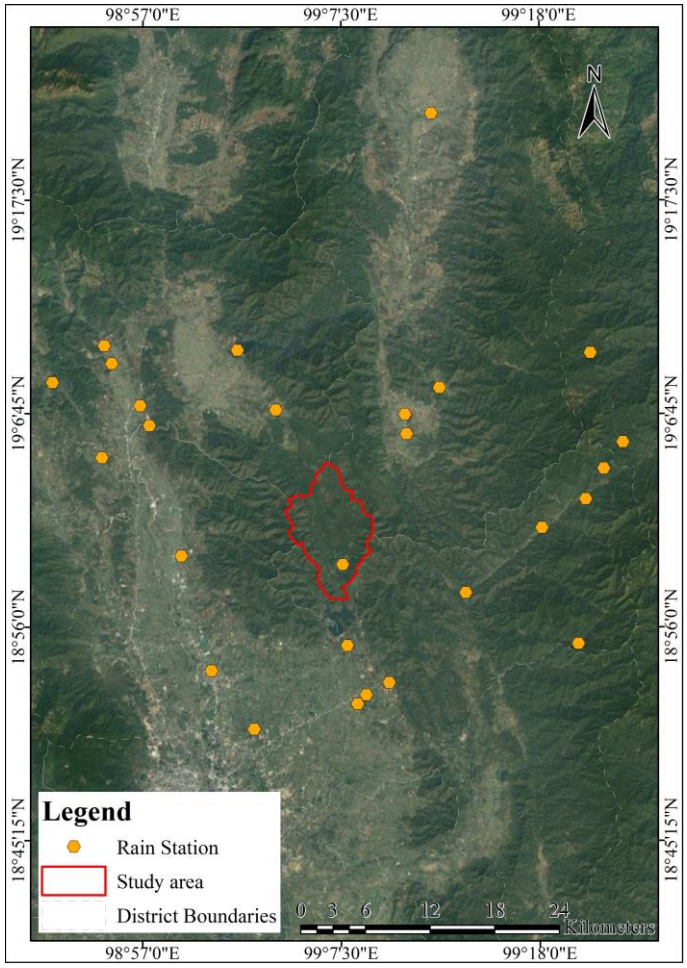

Figure 2: Spatial distribution of meteorology stations used in the study

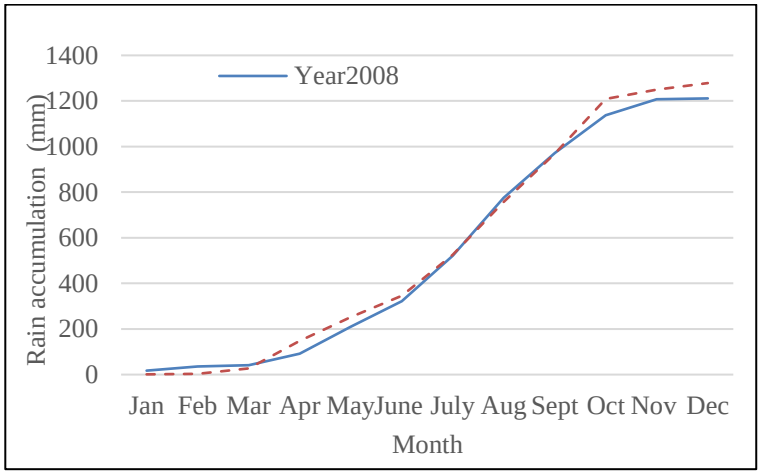

Figure 3: Accumulated rainfall during the study period

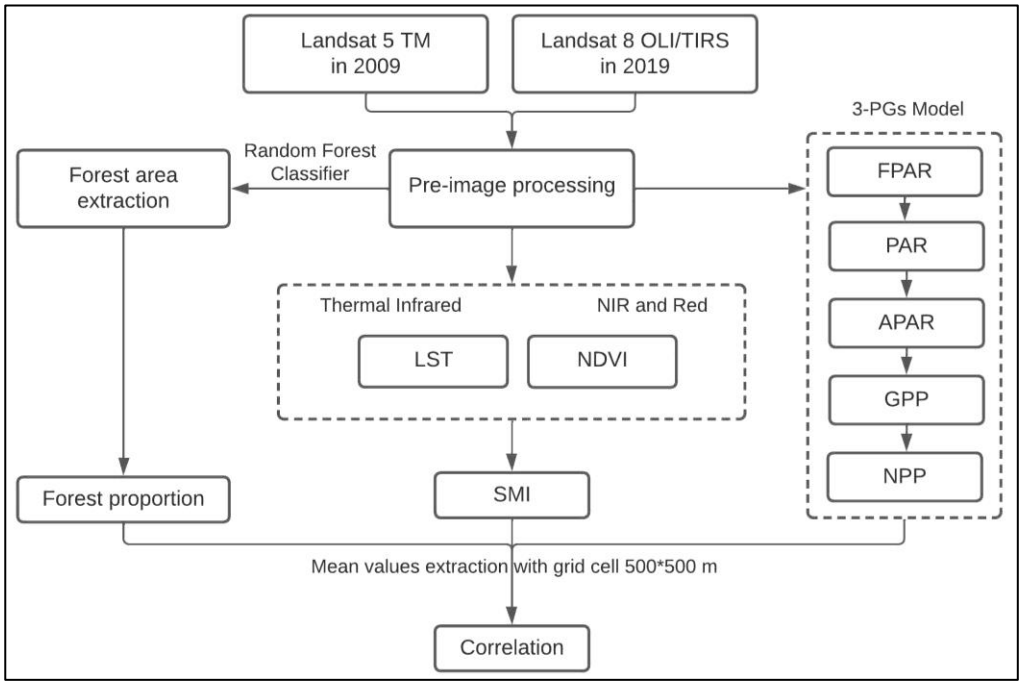

Figure 4: The conceptual framework of this study

3.2.1Forest proportion

The proportion of forest area is calculated by constructing a test grid of 500 m x 500 m across the area and overlapping it with each year's land cover, then calculating the forest area to the total area within the test grid to know the forest area proportion (Figure 5). Each grid boundary was then retrieved for SMI and NPP by extracting the mean within the boundary area. Then take those values to assess the Pearson's correlation coefficient. Before performing the correlation, forest area was extracted using RF classification. The RF classifier has been widely used in the remote sensing which is one of machine learning technique that is used to classify data into different categories. It is based on the idea of using a "forest" of decision trees to make a classification, where each tree in the forest is a decision tree that has been trained on a randomly selected subset of the data.

The final classification is determined by taking the mode (most common) value of the classifications made by each tree in the forest. The RF method is often used in land cover classification because it can improve the accuracy of the classification compared to other methods [27] and [28]. In this study, the RF method was used to classify land cover in Pa Sak Ngam, and the classification accuracy was validated using 100 sampling points and a confusion matrix.

The following process was to compare the correlation of forest area proportion, SMI, and NPP for both years to study the coherence of forest ecosystem management, focusing on changing the forest area.

3.2.2 SMI calculation

There are many methods for studying soil moisture from satellite images. One is the trapezoid method, which examines the relationship between LST and NDVI, whether it is the study by [29] [30] and [31]. The first step in the procedure was to analyze the NDVI using equation 1:

$$\mathrm{NDVI} = \frac{\mathrm{NIR} - \mathrm{RED}}{\mathrm{NIR} + \mathrm{RED}}$$

Equation 1

Where NIR is the reflectance value of the near infrared band, RED is the reflectance value of the red band. The surface temperature was then measured using thermal infrared band of Landsat 5 band 6 (10.40 – 12.50 µm) and Landsat 8 band 10 (10.6 – 11.19 µm). The following equation (equation 2) transforms digital number data to spectral radiance (TOA Radiance Conversion):

$$L_\lambda = M_L Q_{cal} + A_L$$

Equation 2

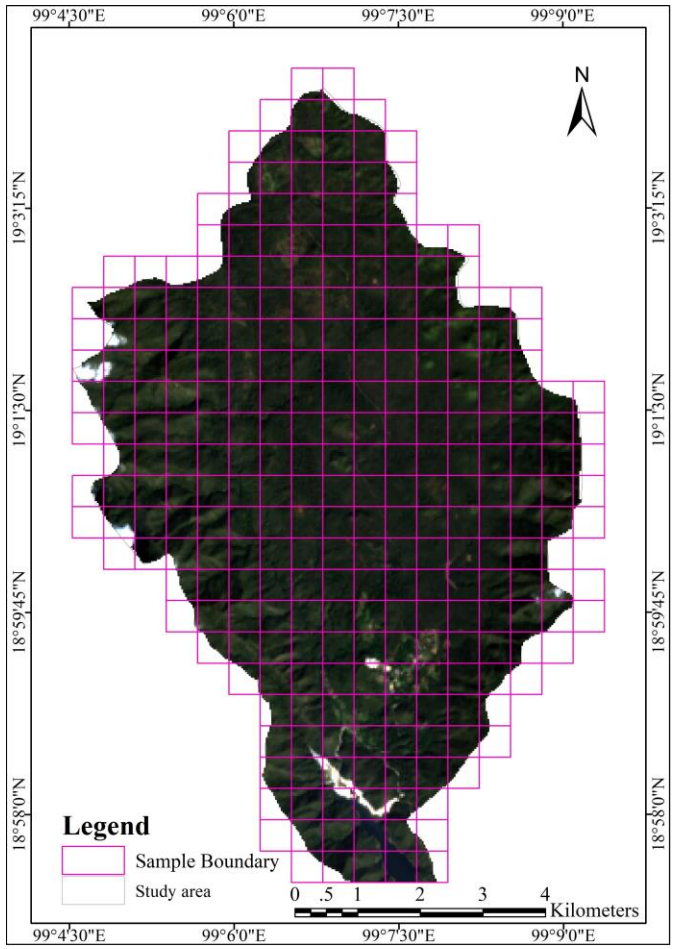

Figure 5: Grid cell map for forest proportion calculation with 500 m x 500 m

Where L_λ is TOA spectral radiance (Watts/(m^2 x srad x μm)) M_L is band-specific multiplicative rescaling factor from the metadata, A_L is band-specific additive rescaling factor from the metadata, and Q_{cal} is quantized and calibrated standard product pixel values (DN). Conversion to top of atmosphere brightness temperature then thermal band data can be converted from spectral radiance to top of atmosphere brightness temperature using the thermal constants as equation 3:

$$T = \frac{K_2}{\ln(\frac{K_1}{L_\lambda}+1)} - 273.15$$

Equation 3

Where T is top of atmosphere brightness temperature (degree Celsius), L_λ is TOA spectral radiance (Watts / (m^2 x srad x μm)), K1, K2 are band-specific thermal conversion constants from the metadata. The next step is to determine soil moisture using SMI. The SMI values have a data range of 0 to 1, with values approaching 0 indicating low soil moisture and approaching 1 indicating high soil moisture [14]. The SMI is calculated from equation 4 as follows:

$$SMI = \frac{LST_{max} - LST}{LST_{max} - LST_{min}}$$

Equation 4

where LST_{max} and LST_{min} are the maximum, and minimum surface temperature for a given NDVI and LST, the surface temperature of a pixel for a given NDVI derived using remotely sensed data. LST_{max} and LST_{min} were calculated using the following equation [32]:

$$LST_{max} = a1 \times NDVI + b1$$

Equation 5

$$LST_{min} = a2 \times NDVI + b2$$

Equation 6

Where LST_{max} is the maximum surface temperature (°C), LST_{min} is the minimum surface temperature (°C), a1, a2, b1, and b2 are the empirical parameters obtained by the linear regression (a present slope and b present intercept) defining both dry and wet (warm and cold) edges of the data (Figure 6).

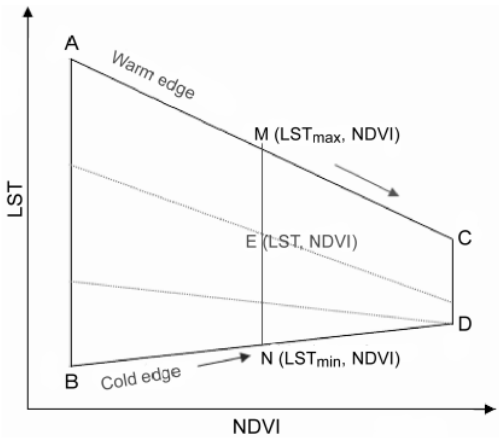

Figure 6: The scatterplot in LST-NDVI space [22]

3.2.3 NPP analysis

The NPP analysis was based on using remote sensing data in conjunction with the 3-PG model. The 3-PG model is used in various fields to predict plant growth and calculate the NPP analysis was based on using remote sensing data in conjunction with the 3-PG model [9] and [11]. There are six steps in the analysis of NPP as follows:

1. The first step is to analyze the NDVI mentioned in the equation 1.
2. The calculation of Fraction of Photosynthetically Active Radiation (FPAR) can be calculated from equation as follow:

$$FPAR = -0.1 + (1.5\text{xNDVI})$$

Equation 7

3. Calculation of Photosynthetically Active Radiation (PAR). This PAR value varies according to the nature of the atmosphere, cloud cover, and the sun's angle and can be calculated from equation as follow:

$$PAR = 0.45 \text{ x Solar radiation}$$

Equation 8

The Solar radiation values were calculated using the Area Solar Radiation apparatus in geospatial programs in MJ/m²/day.

4. Absorption of Photosynthetically Active Radiation (APAR, MJ/m²/day) can be calculated from equation as follow:

$$APAR = FPAR \; x \; PAR$$

Equation 9

5. Gross Primary Productivity (GPP, gC/ m²/day) is the total ratio of carbon produced by plants through photosynthesis. It can be calculated from equation as follow:

$$GPP = 1.80 \frac{g}{MJ} x \; APAR$$

Equation 10

6. Calculation of Net Primary Productivity (NPP, gC/m²/day) is the net ratio of carbon remaining from respiration and photosynthesis of plants as a value for net carbon storage in plants' stems, leaves, and roots. This variable indicates plant growth and fertility and can be calculated from the equation as follow:

$$NPP = 0.47 \text{ x GPP}$$

Equation 11

3.2.4 Correlation analysis

Correlation analysis was used to analyze the relationship between Forest Proportion, SMI and NPP. All those values were extracted with each grid cell boundary and then compared with the correlation coefficient in the same period to analyze the response of SMI and NPP variation to Forest Proportion area using the formula as follows:

$$r = \frac{\sum(x_i - \bar{x})(y_i - \bar{y})}{\sqrt{\sum(x_i - \bar{x})^2 \sum(y_i - \bar{y})^2}}$$

Equation 12

Where r is the correlation coefficient, x_i is values of the x-variable in a sample, $\bar{x}$ is mean of the values of the x-variable, y_i is values of the y-variable in a sample and $\bar{y}$ is mean of the values of the y-variable.

The correlation coefficient measures the strength and direction of a linear relationship between two variables. It ranges from -1 to +1, with -1 indicating a perfect negative correlation (as one variable increases, the other decreases), +1 indicating a perfect positive correlation (as one variable increases, the other increases), and 0 indicating no correlation between the variables. The range of correlation coefficient values and their corresponding levels of correlation are as follows:

very strong positive (0.80 to 1.00), strong positive (0.60 to 0.79), moderate positive (0.40 to 0.59), weak positive (0.20 to 0.39), and very weak positive (0.00 to 0.19) [33].

4. Results and Discussion

The results of this study were divided into 2 areas: the results of the 2009 and 2019 land cover classification and the analysis of the relationship of proportion of forest area, SMI and NPP, with details as follows.

4.1 Classification of land cover 2009and 2019

In 2009 and 2019, the land cover of the study area was divided into three categories: forest, non-forest, and water body. The classification was carried out using the RF classifier and the area of each class was computed by counting class pixels.

After that, the classification's accuracy was determined using an accuracy assessment and the kappa coefficient. The classification accuracy of both years for land cover was the same as 93.8%. However, the kappa coefficient in 2019 was slightly lower than in 2009, with a value of 0.784 compared to 0.800. This shows that while the classification accuracy was comparable between the two years, there may have been a modest decline in the level of agreement between classified and reference data in 2019 compared to 2009. Figure 7 and Figure 8 show land cover statistics and spatial distribution of land use land cover between 2009 and 2019. In 2009, 49,059 km^2 were designated as forest, 8,292 km^2 as non-forest, and 0.49 km^2 as water. In 2019, there were 53,817 km^2 of forest, 3,429 km^2 of non-forest, and 0.598 km^2 of water. Between the two years, the data indicates an increase in forest area and a decrease in non-forest and water areas.

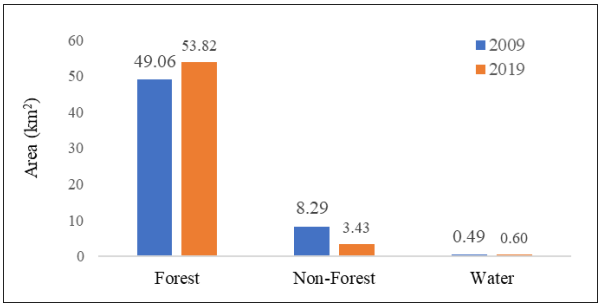

Figure 7: Areas of land cover types in 2009 and 2019

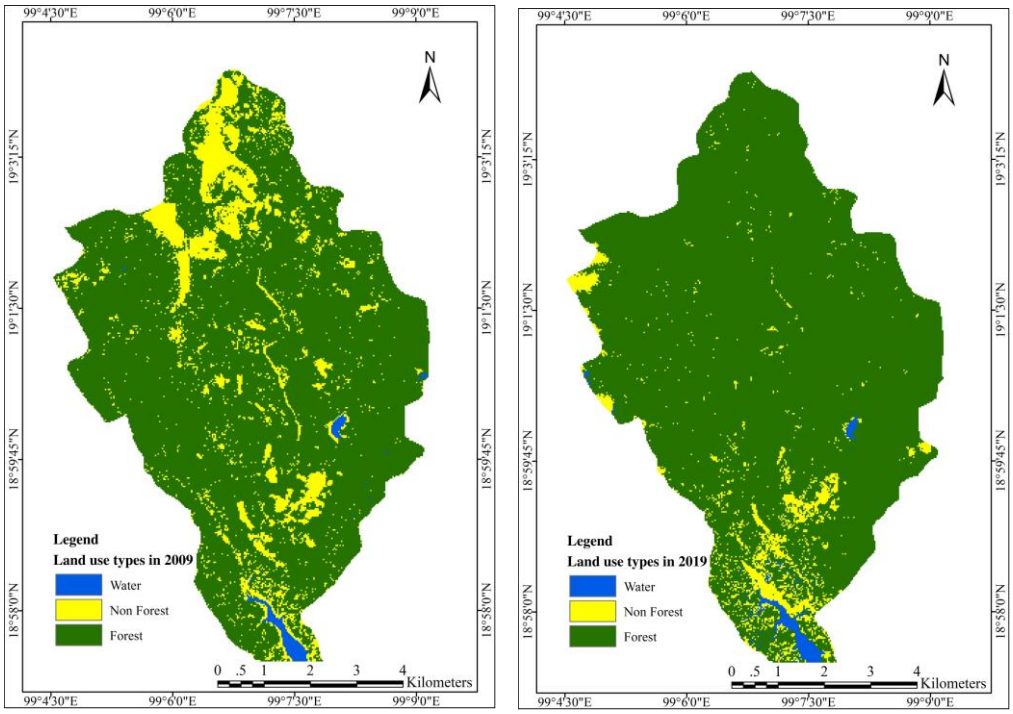

(a) (b)

Figure 8: Result of random forest classification (a) Jan 17, 2009, and (b) Jan 13, 2019

4.2 The Relationship between the Forest Proportion, SMI and NPP

Figures 9, 10 and 11 present the distribution of NPP, SMI, and forest proportion respectively in the study area. Besides, Table 1 demonstrates the NPP, SMI, and proportion of forest area for 2009 and 2019. As demonstrated in Figures 9 and 11, the results of NPP and SMI tend to decrease with increasing slope. This trend is represented by the presence of stripe patterns in the eastern and western regions. Moreover, many study reported that slope can affect the distribution of water, nutrients, and sunlight, which are crucial for plant growth and microbial activity. Steep slopes can lead to soil erosion, which can result in a loss of topsoil and nutrient-rich organic matter, and this can negatively impact NPP and SMI. Furthermore, on steep slopes, water tends to drain more quickly, leading to drier soil conditions and reduced water availability, which can further decrease NPP and SMI [34] [35] and [36]. On the other hand, gentle slopes tend to have better soil stability, and water is more likely to be retained in the soil, providing a more favorable environment for plant growth and microbial activity. In addition, the aspect of a slope, or its orientation towards the sun, can affect the amount and intensity of solar radiation, which can influence photosynthesis rates in plants. Therefore, the slope of a terrain is another critical environmental factor that should be considered when studying the relationship between elevation and ecosystem productivity and function.

Table 1: Statistical of used variables in Pa Sak Ngam village, Luang Nuea sub-district, Doi Saket district, Chiang Mai Province, Thailand

Year	Variable	Max	Min	Mean	Std. Deviation
2009	NPP (gC/m²/day)	6.087	4.133	5.360	0.363
	SMI (no unit, value range between -1 and 1)	0.423	0.036	0.273	0.064
	Proportion of forest area (%)	100	10.380	85.583	19.153
2019	NPP (gC/m²/day)	6.381	4.200	5.634	0.327
	SMI (no unit, value range between -1 and 1)	0.517	0.171	0.346	0.069
	Proportion of forest area (%)	100	4.762	92.349	15.971

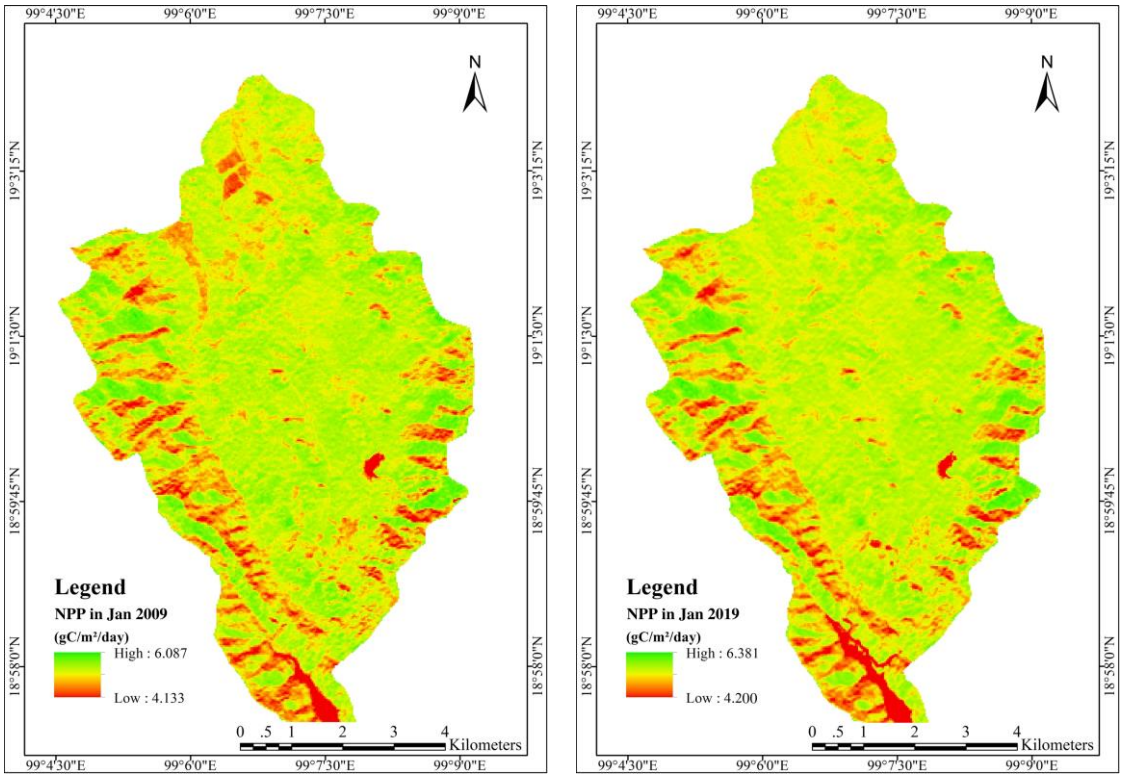

(a) (b)

Figure 9: NPP in (a) 2009 and (b) 2019

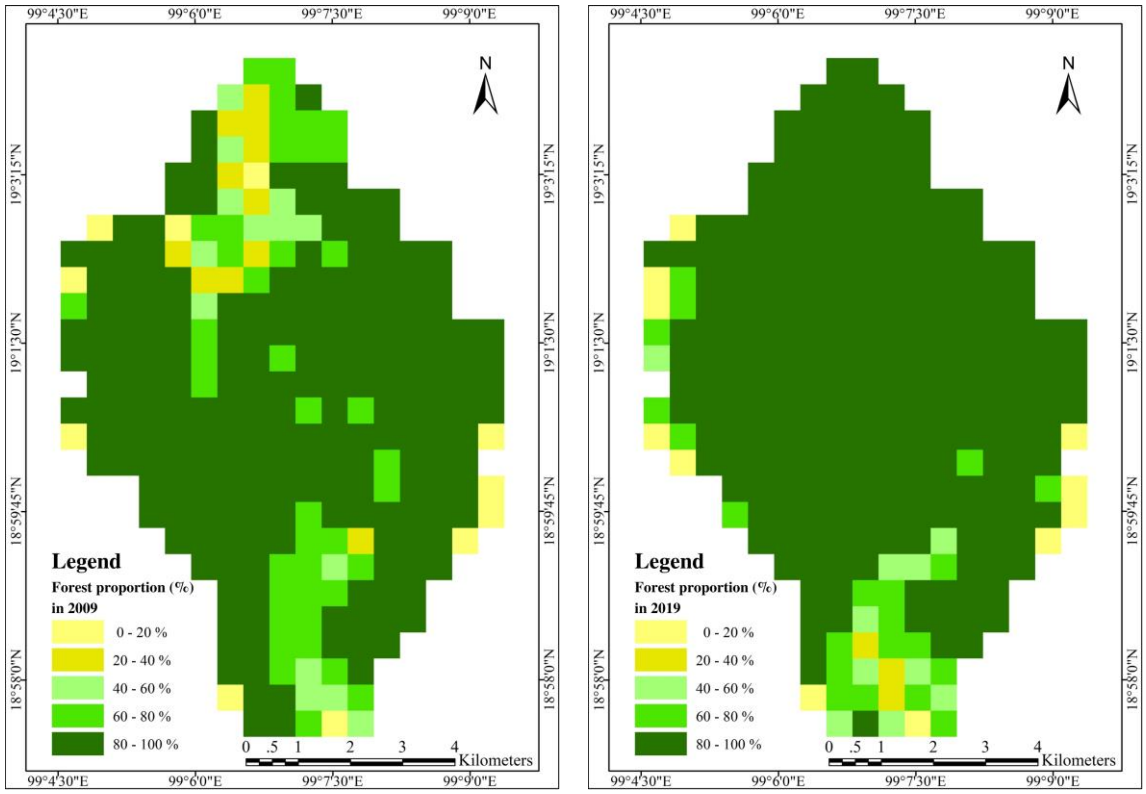

(a) (b)

Figure 10: Percentage of proportion of forest area in (a) 2009 and (b) 2019

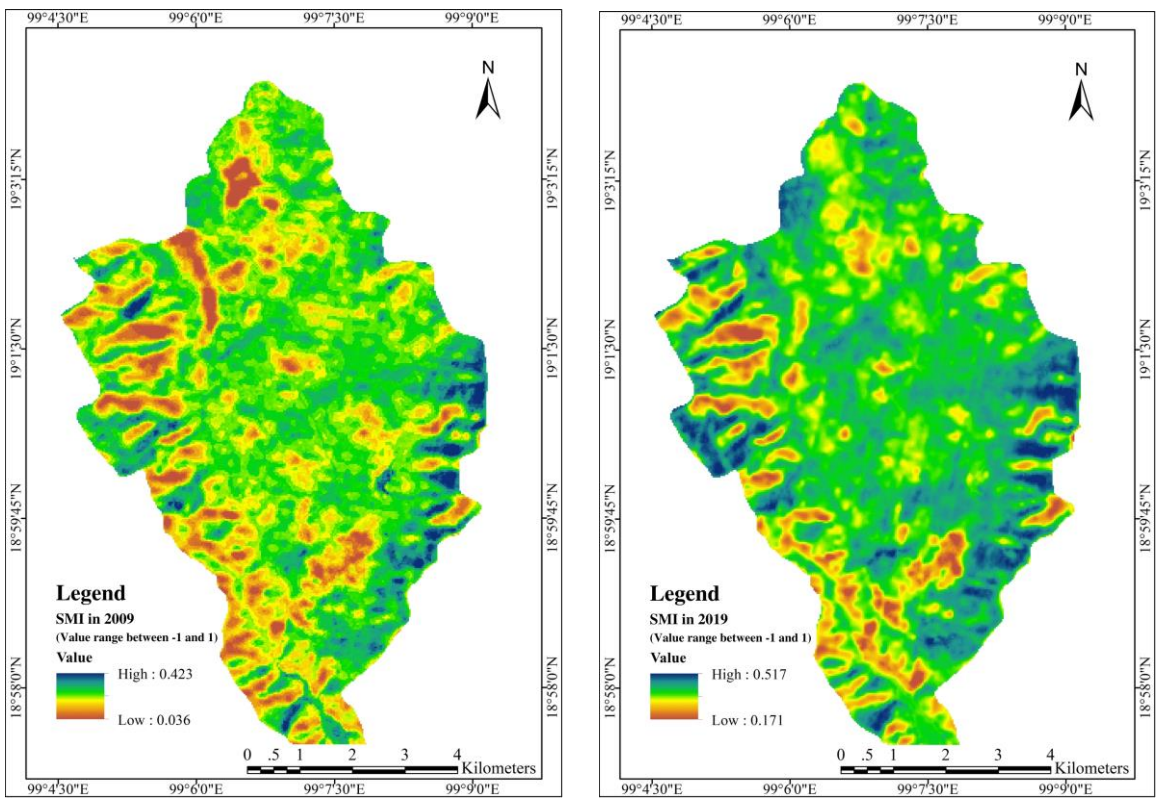

(a) (b)

Figure 11: SMI in (a) 2009 and (b) 2019

Comparing the total rainfall accumulation for the region from January to December for the years 2008 and 2018, the total rainfall accumulation for the region was determined. In 2008, 1211.19 mm of precipitation were measured, whereas in 2018, 1278.46 mm of rainfall were measured. However, it is important to note that the soil moisture variables may be altered by other variables that could explain the variation in soil moisture in the research area over time. When evaluating the data, it is crucial to consider other variables such as soil type, elevation, or slope that may affect the soil moisture.

Scatter plots depicting the relationship between forest proportion and both SMI and NPP in both 2009 and 2019 are presented in Figure 12. Additionally, Table 2 provides the Pearson correlation coefficients (r) between NPP, SMI, and the forest area proportion in 2009 and 2019**.** In 2009, the correlation between NPP and the proportion of forest area was moderate ($r = 0.531$, $p < 0.01$), whereas the correlation between SMI and the proportion of forest area was significant ($r = 0.641$, $p < 0.01$). This shows that NPP and SMI tend to increase as the proportion of forest area increases. For 2019, the correlation between NPP and the proportion of forest area is moderately positive ($r = 0.372$, $p < 0.01$), while the correlation between SMI and the proportion of forest area is weakly positive ($r = 0.322$, $p < 0.01$). This indicates that, while there is still a positive association between NPP and the proportion of forest area, and SMI and the proportion of forest area, the correlation is less than in 2009.

The study found that the relationship between forest area proportion, SMI, and NPP was stronger in 2009 than in 2019. This is likely since in 2009, some areas were being actively planted and restored, resulting in a greater variety of data and a more evident relationship. In contrast, by 2019, the forests had already begun to recover to some extent, leading to more concentrated data with a narrower range and a weaker correlation. However, the correlations were still significant in both years, indicating that the proportion of forest area affects SMI and NPP.

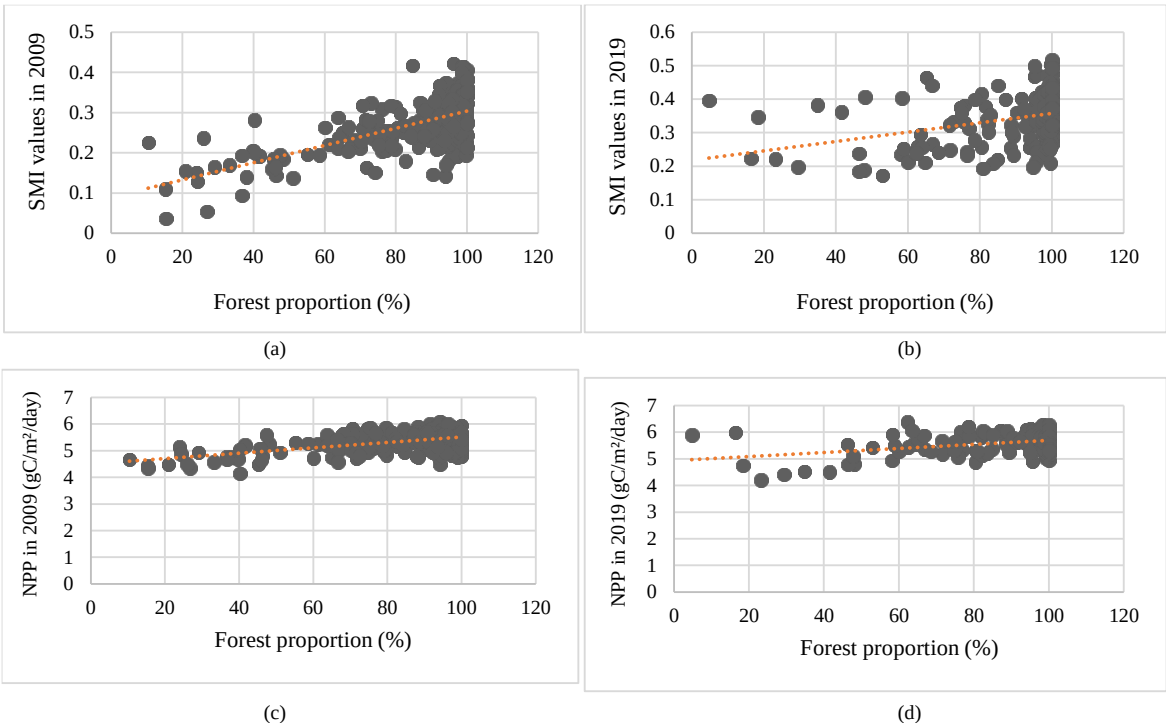

Figure 12: Scatter plot of (a) forest proportion and SMI in 2009, (b) forest proportion and SMI in 2019, (c) forest proportion and NPP in 2009 and (d) forest proportion and NPP in 2019

Table 2: Correlation between forest proportion, SMI and NPP

The proportion of forest area (Percentage)	**Pearson correlation coefficients; r**	
	NPP	**SMI**
2009	0.531^{**}	0.641^{**}
2019	0.372^{**}	0.322^{**}

Nonetheless, correlation does not indicate causation, as other variables, such as temperature, precipitation, and vegetation, may also influence these variables. Additionally, it is essential to investigate different analysis methods and multiple data sources to validate the conclusions.

The findings of the study revealed a positive correlation between the proportion of forest area and NPP, with a moderate correlation coefficient of 0.531 in 2009 and a weak correlation coefficient of 0.372 in 2019. The proportion of forest area, as represented by satellite imagery data, serves as an indicator of the forest canopy area. As the forest canopy increases, there is a corresponding increase in the rate of photosynthesis and food production, thus leading to an elevation of NPP within the ecosystem. However, it is important to note that the data utilized in the study, specifically the proportion of forest area obtained from satellite imagery, is not specific enough to identify the particular lower plants or shrubs responsible for energy production. These results suggest that there is a positive relationship between the proportion of forest area and net primary productivity, albeit with a moderate association in 2009 and a weak correlation in 2019.

5. Conclusion

In this study, the land use of a study area in Pa Sak Ngam village region, Thailand was classified into forest, non-forest, and water body categories for the years 2009 and 2019 using the RF classifier. There was an increase in forest area in 2009 to 2019 due to the reforestation management of upstream forests and the growth of forests, which led to a change in land use. The study also explored the relationship between forest proportion, SMI, and NPP in the area. Landsat images was used to classify the forest area, calculated soil moisture using a soil moisture index, and used the 3-PGs model to compute net primary productivity. The results showed that both NPP and SMI tended to decrease with increasing slope. Finally, the scatter plots and correlation coefficients showed a positive correlation between the forest proportion and both NPP and SMI, indicating that the forest has a positive impact on ecosystem productivity and function. It is important to consider other variables such as soil type, elevation, or slope that may affect soil moisture when interpreting the data.

Acknowledgments

This research was funded by The Thailand Research Fund (TRF) and Chiang Mai University, Thailand. The acknowledgment also goes to NASA for the Landsat series data.

References

[1] Díaz, S., (2013). Ecosystem Function Measurement, Terrestrial Communities, in *Encyclopedia of Biodiversity (Second Edition)*, S. A. Levin, Ed. Waltham: Academic Press. 72-89. https://doi.org/10.1016/B978-0-12-384719-5.00042-3

[2] Fensholt, R., Langanke, T., Rasmussen, K., Reenberg, A., Prince, S. D., Tucker, C., Scholes, R. J., Le, Q. B., Bondeau, A., Eastman, R., Epstein, H., Gaughan, A. E., Hellden, U., Mbow, C., Olsson, L., Paruelo, J., Schweitzer, C., Seaquist, J. and Wessels, K. (2012). Greenness in Semi-Arid Areas Across the Globe 1981–2007 — an Earth Observing Satellite Based Analysis of Trends and Drivers, *Remote Sensing of Environment*, Vol. 121, 144-158. https://doi.org /10.1016/j.rse.2012.01.017.

[3] Piao, S., Ciais, P., Huang, Y., Shen, Z., Peng, S., Li, J., Zhou, L., Liu, H., Ma, Y., Ding, Y., Friedlingstein, P., Liu, C., Tan, K., Yu, Y., Zhang, T. and Fang, J., (2010). The Impacts of Climate Change on Water Resources and Agriculture in China, *Nature*, Vol. 467(7311), 43-51. https://doi.org/10.1038/nature09364.

[4] Liu, L., Gudmundsson, L., Hauser, M., Qin, D., Li, S. and Seneviratne, S. I., (2020). Soil Moisture Dominates Dryness Stress on Ecosystem Production Globally, *Nature Communications*, Vol. 11(1), https://doi.org/10.1038/s41467-020-18631-1.

[5] Yue, D., Zhou, Y., Guo, J., Chao, Z. and Guo, X., (2022). Relationship between Net Primary Productivity and Soil Water Content in the Shule River Basin. *CATENA*, Vol. 208, https://doi.org /10.1016/j.catena.2021.105770

[6] Chen, J., Shao, Z., Huang, X., Zhuang, Q., Dang, C., Cai, B., Zheng, X. and Ding, Q., (2022). Assessing the Impact of Drought-Land Cover Change on Global Vegetation Greenness and Productivity. *Science of the Total Environment*, Vol. 852, https://doi.org/10.1016/j.scitotenv.20 22.158499.

[7] Zeng, B., Zhang, F., Wei, L., Zhang, X. and Yang, T., (2021). An Improved IBIS Model for Simulating NPP Dynamics in Alpine Mountain Ecosystems: A Case Study in the Eastern Qilian Mountains, Northeastern Tibetan Plateau, *CATENA*, Vol. 206. https://doi.org/10.1016/j.catena.2021.105479.

[8] Dokulil, M. and Gross, T., (2019). Net Production in Different Environments. *Encyclopedia of Ecology (Second Edition)*, B. Fath, Ed. Oxford: Elsevier. 34-345.

https://doi.org/10.1016/B978-0-12-409548 9.108 91-7

[9] Landsberg, J. and Sands, P., (2011). Chapter 9 - The 3-PG Process-Based Model. *Terrestrial Ecology*, Vol. 4, 241-282. https://doi.org/10.1016/B978-0-12-3744609.000 09-3.

[10] Forrester, D. I. and Tang, X., (2016). Analysing the Spatial and Temporal Dynamics of Species Interactions in Mixed-Species Forests and the Effects of Stand Density Using the 3-PG Model, *Ecological Modelling*, Vol. 319, 233-254. https://doi.org/10.1016/j.ecolmodel.2015.07.010.

[11] Nightingale, J. M., Hill, M. J., Phinn, S. R., Davies, I. D., Held, A. A. and Erskine, P. D., (2008). Use of 3-PG and 3-PGS to Simulate Forest Growth Dynamics of Australian Tropical Rainforests: I. Parameterisation and Calibration for Old-Growth, Regenerating and Plantation Forests, *Forest Ecology and Management*, Vol. 254(2), 107-121. https://doi.org/10.1016/j.foreco .2007.03.041.

[12]Prangkio, C., Malumpong, C., Charoenpanyanet, A., Pongleerat, S. and Khamnonkhom, P., (2009). Integration of Satellite Imagery Data with 3PGs Model for Assessment of Forest Productivity. *Journal of Remote Sensing and GIS Association of Thailand*, Vol. 10(2). 23-32.

[13] Sangngam, C. and Charoenpanyanet, A., (2016). Estimation of Above-ground Carbon Sequestration of Para Rubber Based on Satellite Imageries Using CASA-biosphere Model. *Journal of Remote Sensing and GIS Association of Thailand*, Vol. 17. 109-120.

[14]Moawad, B., (2012). *Geoscience General Tool Package*. Max-Planck Institute fürChemie, Mainz, Germany.

[15]Guha, S. and Govil, H., (2020). Land Surface Temperature and Normalized Difference Vegetation Index Relationship: A Seasonal Study on a Tropical City. *SN Applied Sciences*, Vol. 2(10). https://doi.org/10.1007/s42452-020-03458-8.

[16]Sun, D. and Kafatos, M., (2007). Note on the NDVI-LST Relationship and the Use of Temperature-Related Drought Indices Over North America. *Geophysical Research Letters*, Vol. 34(24). https://doi.org/10.1029/2007GL 031485.

[17]Yue, W., Xu, J., Tan, W. and Xu, L., (2007). The Relationship between Land Surface Temperature and NDVI with Remote Sensing: Application to Shanghai Landsat 7 ETM+ Data. *International Journal of Remote Sensing*, Vol. 28(15), 3205-3226. https://doi.org/10.1080/01431160500306906.

[18]Pa Sak Ngam Community (2011). *Pa Sak Ngam Community Manual for Check Dams*. Hydro-Informatics Institute of Ministry of Higher Education, Science, Research and Innovation in Thailand.

[19]Bronowicka-Mielniczuk, U., Mielniczuk, J., Obroślak, R. and Przystupa, W., (2019). A Comparison of Some Interpolation Techniques for Determining Spatial Distribution of Nitrogen Compounds in Groundwater. *International Journal of Environmental Research*, Vol. 13(4), 679-687. https://doi.org/10.1007/s41742-019-00208-6.

[20] Yang, X., Xie, X., Liu, D. L., Ji, F. and Wang, L., (2015). Spatial Interpolation of Daily Rainfall Data for Local Climate Impact Assessment over Greater Sydney Region. *Advances in Meteorology*, Vol. 2015. https://doi.org/10.1155 /2015/563629.

[21]Keskin, M., Dogru, A. O., Balcik, F. B., Goksel, C., Ulugtekin, N. and Sozen, S., (2015). Comparing Spatial Interpolation Methods for Mapping Meteorological Data in Turkey. *Energy Systems and Management*, Springer International Publishing, 33-42. https://doi/org/10.1007/978-3-319-16024-5_3.

[22]Bessinger, M., Lück-Vogel, M., Skowno, A. and Conrad, F., (2022). Landsat-8 Based Coastal Ecosystem Mapping in South Africa Using Random Forest Classification in Google Earth Engine. *South African Journal of Botany*, Vol. 150, 928-939. https://doi.org/10.1016/j.sajb.2 022.08.014.

[23]Billah, M., Islam, A. K. M. S., Mamoon, W. B. and Rahman, M. R., (2023). Random Forest Classifications for Landuse Mapping to Assess Rapid Flood Damage Using Sentinel-1 and Sentinel-2 Data. *Remote Sensing Applications: Society and Environment*, Vol. 30, https://doi.org/ 10.1016/j.rsase.2023.100947.

[24]Jonathan, L., Adeline, F., Andyne, L., Céline, P. and Hugues, C., (2022). Prediction of Forest Nutrient and Moisture Regimes from Understory Vegetation with Random Forest Classification Models. *Ecological Indicators*, Vol. 144. https://doi.org/10.1016/j.ecolind.2022.109446.

[25]Belgiu, M. and Drăguţ, L., (2016). Random Forest in Remote Sensing: A review of Applications and Future Directions. *ISPRS Journal of Photogrammetry and Remote Sensing*, Vol. 114, 24-31. https://doi.org/10.1016/j.isprs jprs.2016.01.011.

[26]Breiman, L. J. M. l., (2001). Random Forests. *Machine Learning*, Vol. 45, 5-32.

[27]Gibson, R., Danaher, T., Hehir, W. and Collins, L., (2020). A Remote Sensing Approach to Mapping Fire Severity in South-Eastern Australia Using Sentinel 2 and Random Forest. *Remote Sensing of Environment*, Vol. 240. https://doi.org /10.1016/j.rse.2020.111702.

[28]Meng, Y., Yang, M., Liu, S., Mou, Y., Peng, C. and Zhou, X., (2021). Quantitative Assessment of the Importance of Bio-Physical Drivers of Land Cover change Based on a Random Forest Method, *Ecological Informatics*, Vol. 61. https://doi.org/10.1016/j.ecoinf.2020.101204

[29]Yang, Y., Guan, H., Long, D., Liu, B., Qin, G., Qin, J. and Batelaan, O., (2015). Estimation of Surface Soil Moisture from Thermal Infrared Remote Sensing Using an Improved Trapezoid Method. *Remote Sensing*, Vol. 7(7), 8250-8270. https://doi.org/10.3390/rs70708250.

[30]Wang, W., Huang, D., Wang, X. G., Liu, Y. R. and Zhou, F., (2010). Estimate Soil Moisture Using trapezoidal Relationship between Remotely Sensed Land Surface Temperature and Vegetation Index. *Hydrology and Earth System Sciences Discussions*, Vol. 15(5), 1699–1712. https://doi.org/10.5194/hess-15-1699-2011

[31]Potić, I., Bugarski, M. and Matić-Varenica, J., (2017). Soil Moisture Determination Using Remote Sensing Data for the Property Protection and Increase of Agriculture Production. *The Egyptian Journal of Remote Sensing and Space Scienc*e, Vol. 23(3), 347-353, https://doi.org/ 10.1016/j.ejrs.2019.04.003.

[32]Parida, B., Collado, W., Borah, R., Hazarika, M. and Samarakoon, L., (2008). Detecting Drought-Prone Areas of Rice Agriculture Using a MODIS-Derived Soil Moisture Index. *GIScience & Remote Sensing*, Vol. 45(1), 109-129. https://doi. org/10.2747/1548-1603.45.1.109.

[33]Meghanathan, N., (2016). Assortativity Analysis of Real-World Network Graphs based on Centrality Metrics. *Computer and Information Science*, Vol. 9(3), 7-25. http://dx.doi.org/10. 5539/cis.v9n3p7.

[34]Elnaker, N. and Zaleski, T., (2021). *The Impact of Slope Aspect on Soil Temperature and Water Content*. International Symposium on Soil Science and Plant Nutrition. Samsun, Turkey.

[35]Shan, Y., Xie, J., Lei, N. and Dong, Q., (2020). Soil Moisture Characteristics of a Typical Slope in the Watershed of the Loess Plateau for Gully Land Consolidation Project. *E3S Web of Conferences*, Vol. 199. https://doi.org/10.1051/ e3sconf/202019900006.

[36]Guo, Q., Cheng, S., Qin, W., Ning, D., Shan, Z. and Yin, Z., (2020). Vertical Variation and Temporal Trends of Extreme Precipitation Indices in a Complex Topographical Watershed in the Hengduan Mountain Region, China. *International Journal of Climatology*, Vol. 40(6), 3250-3267. https://doi.org/10.1002/joc.6395.